

Nitrogen-rich indium nitride

K. S. A. Butcher,^{a)} M. Wintrebert-Fouquet, P. P.-T. Chen, T. L. Tansley, and H. Dou
Physics Department, Macquarie University, Sydney NSW 2109, Australia

S. K. Shrestha and H. Timmers^{b)}
School of Physics, University of New South Wales at the Australian Defence Force Academy, Canberra, ACT 2600, Australia

M. Kuball
H. H. Wills Physics Laboratory, University of Bristol, Bristol BS8 1TL, United Kingdom

K. E. Prince
Australian Nuclear Science and Technology Organisation, Private Mail Bag 1, Menai NSW 2234, Australia

J. E. Bradby
Department of Electronic Materials Engineering, Research School of Physical Sciences and Engineering, The Australian National University, Canberra, ACT 0200, Australia

(Received 24 July 2003; accepted 1 March 2004)

Elastic recoil detection analysis, using an incident beam of 200 MeV Au ions, has been used to measure indium nitride films grown by radio-frequency sputtering. It is shown that the films have nitrogen-rich stoichiometry. Nitrogen vacancies are therefore unlikely to be responsible for the commonly observed high background carrier concentration. Ultraviolet Raman and secondary ion mass spectroscopy measurements are used to probe the state of the excess nitrogen. The nitrogen on indium anti-site defect is implicated, though other possibilities for the site of the excess nitrogen, such as molecular nitrogen, or di-nitrogen interstitials cannot be excluded. It is further shown that a shift in the (0002) x-ray diffraction peak correlates with the excess nitrogen, but not with the oxygen observed in some samples. © 2004 American Institute of Physics.

[DOI: 10.1063/1.1711173]

I. INTRODUCTION

At present, many of the fundamental properties of InN are not well known: there is considerable debate over the band gap of InN,¹⁻⁴ and there has been very little experimental study of the materials defect structure. The highest mobility indium nitride ever produced had a high room temperature value of 2700 cm²/V s for an electron concentration of 5×10^{16} cm⁻³.⁵ However even this material was heavily compensated. A predicted maximum theoretical room temperature mobility of 4400 cm²/V s⁶ indicates approximately 60% compensation of the primary donor in that material. This suggests that the microstructure of InN is defect dominated. The source of the high density of background *n*-type carriers commonly observed for this material is also unknown. Various theoretical assessments, not experimentally confirmed, suggest that the high electron carrier concentration has four possible sources: (i) oxygen atoms on nitrogen sites;⁷ (ii) silicon atoms on indium atom sites;⁷ (iii) hydrogen incorporation;⁸ or (iv) nitrogen vacancies.⁹ We note that defect complexes may also be significant.

The long-standing presumption that indium nitride is inevitably grown with a high level of nitrogen vacancies is encompassed in all past reviews of the material, and derives from the requirement of high nitrogen overpressure to pre-

vent decomposition and nitrogen loss at relatively moderate temperatures compared to gallium nitride. Despite there being significant variability in the decomposition values reported for indium nitride,¹⁰ this material should be nitrogen deficient when grown under conditions of thermodynamic equilibrium. We carried out elastic recoil detection (ERD) analysis of the InN films using 200 MeV Au ions to test the hypothesis of nitrogen deficiency, and were surprised by the high levels of excess nitrogen that were found.

II. EXPERIMENT

The samples examined here were polycrystalline films grown by rf sputtering, the same method used to produce the highest mobility nitride material ever grown,⁵ though only high electron carrier concentration material ($> 10^{19}$ cm⁻³) was used in this study. ERD analysis results for MBE grown material are presented elsewhere⁴ though an example of an UV Raman spectrum for a MBE sample grown by Cornell University is provided here. No sample heating was used during film growth for the rf sputtered samples, though measurements indicate that samples typically reach a temperature of <30 °C during sputtering. The growth periods used were 1 to 2 days and all the films were grown on borosilicate glass degraded prior to loading in the growth system.

The ERD technique¹¹ has proven useful in determining the elemental composition of GaN films,^{12,13} and was readily applied here to determine the N/In ratio of InN films. During the ERD analysis the energy deposited in the films by the

^{a)}Electronic mail: sbutcher@ics.mq.edu.au

^{b)}Also at: Department of Nuclear Physics, Australian National University, Canberra, ACT 0200, Australia.

TABLE I. Band gaps; N/In ratios measured using ERD analysis; *c* axis lattice constants; oxygen and carbon compositions for InN films.

Sample ID	InN sample 1	InN sample 2		InN sample 3
Band gap	2.3 eV	2.27 eV		2.14 eV
N/In	1.31±0.03	1.32±0.04	1.30±0.03	1.14±0.03
<i>c</i> axis lattice parameter calculated from (0002) reflection (Å)	5.792	5.794		5.772
Oxygen content (at. %)	10.7	9.3		9.3
Carbon content (at. %)	0.8	0.8		0.8

incident Au ions caused significant nitrogen depletion of this material. The large detection solid angle of the recoil ion detector,¹⁴ however, enables the depletion to be monitored *in situ* as a function of the Au ion fluence. A suitable depletion model has been demonstrated^{15,16} to allow reliable extrapolations of the experimental data back to zero fluence so that N/In ratios can be determined accurately. Table I shows the N/In ratios measured by ERD for a representative set of films; the smooth energy spectra of the detected indium recoil ions indicate that the N/In ratio does not vary with the film thickness. All samples had values much greater than 1.00 to as high as 1.32. We have shown elsewhere⁴ that thin films of InN grown by MBE can also be very nitrogen rich. It is important to remember that the ERD analysis is for thin samples since it appears that there are substantial improvements in material quality for thicker samples.¹⁷ Both techniques use plasma nitrogen sources and are therefore able to produce films under nonequilibrium conditions. Given that these films appear to be nitrogen rich, nitrogen vacancies are an unlikely source of their donors.

Table I also provides the carbon and oxygen levels present for the films as quantified with ERD analysis. Oxygen incorporation in the present films was relatively high, with an atomic oxygen concentration of approximately 10% being present in the films, but as suggested by Kumar *et al.*¹⁸ the oxygen may reside predominantly at grain boundaries (as was recently shown to be the case for polycrystalline GaN

grown at 570 °C¹²) and result from postgrowth exposure to the ambient.

Also provided in Table I are band gaps measured by UV–Vis transmission spectroscopy and *c*-axis lattice spacings determined from (0002) x-ray diffraction (XRD) reflections, measured with a Phillips PW-1830 system using Cu *kα* x rays. An XRD spectrum typical of the samples of Table I is shown in the lower trace of Fig. 1 with (0002) and (0004) reflections prominent, though as shown in Table I the reflection positions are shifted compared to the standard *c* lattice constant value of 5.700 Å, given by the International Center for Diffraction Data (formerly the Joint Committee on Powder Diffraction Standards). Figure 2 shows the absorption spectra, plotted as absorption coefficient squared versus energy, for the samples of Table I. The cross-sectional transmission electron microscopy (XTEM) samples of the InN on Si layers were prepared using an FEI XP200 focused ion beam system. The samples were then imaged using a Philips CM 300 transmission electron microscope at an operating accelerating voltage of 300 kV. A cross-sectional image is shown in Fig. 3 with the associated columnar polycrystalline structure of the hexagonal film clearly visible. The shift in lattice constant, seen in Table I, is not dependent on oxygen content, which is constant for these samples, but varies with the N/In ratio. This is to be expected when oxygen is resident at grain boundaries and excess nitrogen is embedded in the lattice as a point defect. Interestingly, for GaN, Lagerstedt and Monemar¹⁹ observed a strong increase in lattice parameters that they attributed to self-interstitials in nitrogen-rich material, a case that may be similar to that observed here. Optical

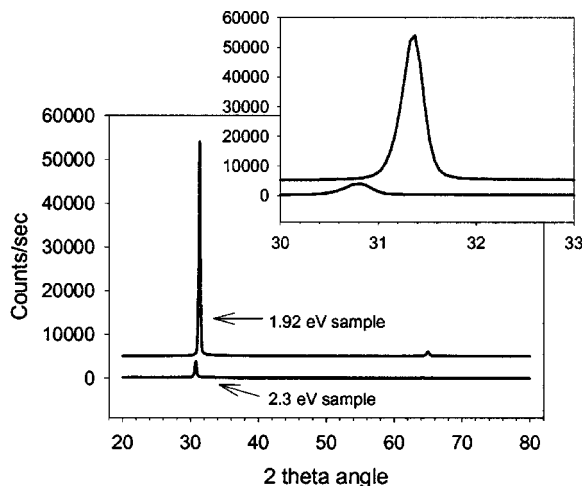


FIG. 1. XRD spectra of 2.3 eV InN sample (lower trace) and of 1.92 eV InN sample (upper trace—offset by 50000 counts/s). The same data are shown focused on the (0002) reflection in the inset.

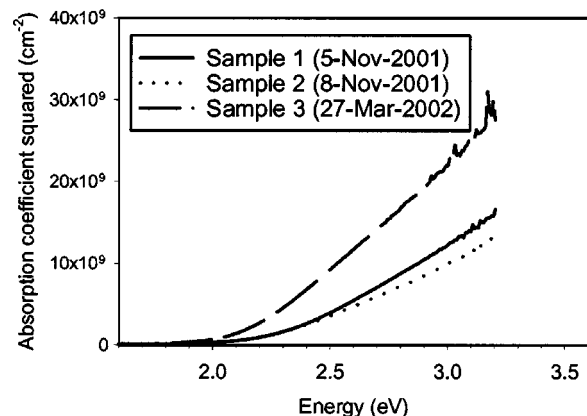


FIG. 2. Absorption coefficient squared vs energy plots, the *x* intercept of the linear portion of the plots provides the band gap of the material.

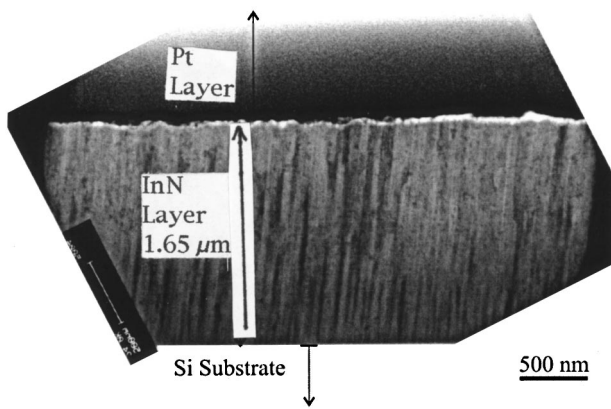


FIG. 3. Bright-field XTEM image of InN cross section with silicon substrate visible at the bottom of the image. The columnar habit of the film is clearly evident.

band gaps included in Table I show the expected dependence on lattice spacing. Samples grown more recently, with 1.92 eV band gap, under less nitrogen-rich growth conditions (evidenced by the band edge and by the secondary ion mass spectroscopy (SIMS) results discussed in the following) are closer to the value of 1.89 eV reported for low electron concentration samples.²⁰ XRD indicates a c lattice constant of 5.699 Å for these samples, a value in agreement with that given by the International Center for Diffraction Data and with recent high resolution measurements made on bulk indium nitride samples.²¹ A sample XRD spectrum is shown in the upper trace of Fig. 1. SIMS indicates these samples have approximately the same oxygen content as the samples of Table I. We conclude that excess nitrogen correlates well with increases in both the c lattice parameter and the optical band gap and that these changes are uncorrelated to the sample oxygen concentration.

III. DEFECT DETERMINATION

The nature of the excess nitrogen has been examined using a Renishaw UV-Raman system. A 325 nm HeCd laser excitation was used in reflection mode to observe phonons related to chemical bonding. Figure 4(a) shows a typical Raman spectrum obtained for one of the rf sputtered InN films of Table I. The broad quartz peak is believed to be due to the silica optical components of the measurement system. The spectrum shows InN related phonons at 400–700 cm^{-1} while N–N bonding is evident at 2200–2350 cm^{-1} . The low carbon content for these films (Table I) eliminates the possibility of C–N triple bonds in the same wave-number range as N–N bonds. The 2200–2350 cm^{-1} peak is also too broad to be due to nitrogen gas (occasionally seen with an UV laser source), rather it shares with the In–N phonon peaks a similar broadening—in this case determined either by the polycrystallinity of the film, or by local site related variations in the bonding structure of the N–N species. The peak is therefore due to N–N bonding in the sample and is indicative of the type of native defect present. The 2200–2350 cm^{-1} peak supports the assignment of the excess nitrogen to a nitrogen on indium (N_{In}) anti-site defect, or alternately to the presence of molecular nitrogen distributed in the lattice since

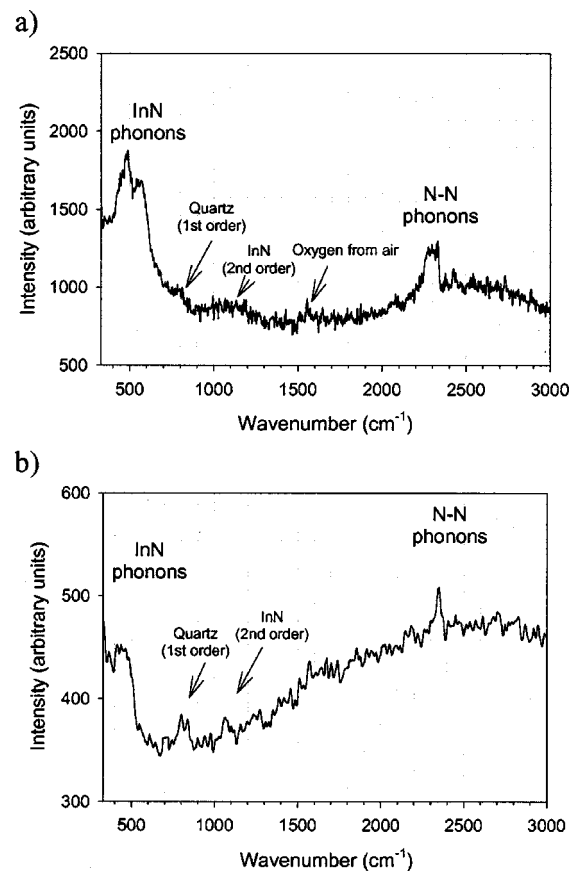


FIG. 4. (a) UV reflection mode Raman spectrum of a rf sputtered InN sample with In–N and N–N bonding states evident. (b) UV reflection mode Raman spectrum of an MBE grown InN (Cornell sample GS-1311), this spectrum also shows In–N and N–N bonding states.

N–N bonding would be present for both such defects. A di-nitrogen interstitial complex may also be a possibility,²² though there have been no theoretical calculations for such a complex in InN. Based on existing thermodynamic considerations, one of the most favorable sites for excess nitrogen in InN is as the N_{In} anti-site defect, while the defect formation energy of nitrogen interstitials is not thermodynamically preferred.⁷ The anti-site defect is a double donor with a shallow first-ionization energy level⁷ and is therefore a candidate for the supply of the high background donor concentration. Interestingly, Raman measurements with lower wavelength excitation sources show no evidence of N–N bonding. This indicates that there is either a strong resonance for the N–N structure at the UV excitation wavelength, or alternately it indicates that the N–N bonding is a surface species (since the penetration depth of the UV excitation into the InN is of the order of nanometers). It is therefore possible that the excess nitrogen exists in another state in the bulk of the InN and only forms the N–N bound species at the sample surface. This would be consistent with the model developed to explain dose related nitrogen loss during ERD measurements.¹⁶

Figure 4(b) shows an UV Raman spectrum for a MBE InN sample grown by Cornell University (sample GS-1311, 800 nm of InN on 200 nm of AlN). This sample also shows evidence of N–N bonding, though typically MBE grown

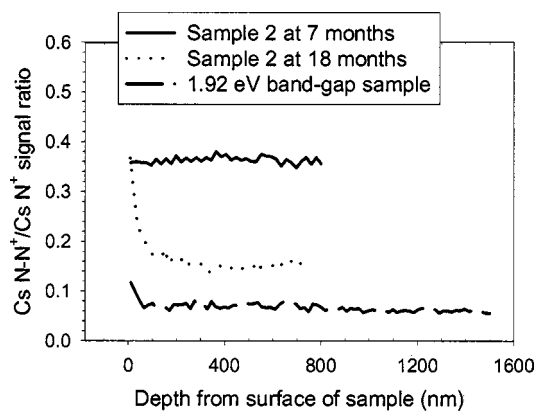


FIG. 5. N–N to atomic N SIMS signal ratios for InN samples.

samples do not show as strong a N–N signal as typical rf sputtered samples, indicating that better stoichiometry is more easily achieved for the MBE samples, as supported by ERD measurements provided elsewhere.⁴

SIMS measurements were carried out using the Cameca 5F dynamic SIMS system of the Australian Nuclear Science and Technology Organization with a Cs^+ ion beam. The methodology of Gao²³ was applied, whereby CsM^+ (where M is the element mass being analyzed) molecules are collected instead of M^+ . The influence of Cs^+ ion beam fluctuation was eliminated by normalizing the collected signals to the average of the Cs^+ ion beam signal. The normalization to Cs^+ was also done as a first-order work function correction, which reduces any yield related matrix effects from the spectrum and thereby allows ease of interpretation of spectra. Using this methodology we were able to detect the excess nitrogen present in the rf sputtered samples, evident as a strong N–N signal (relative to the atomic nitrogen signal) at atomic mass number 28 (subtracting the Cs ion mass number), not due to silicon since that element would have had to have been present at ~ 5 at. % for this signal strength, and yet ERD, an absolute measurement technique, detected no Si in the bulk InN to a detection limit of less than 0.1%. Figure 5 shows the SIMS data for sample 2. Interestingly, after a storage period of 18 months, film blistering was observed for the film (Fig. 6) and the SIMS signal for the N–N bonding in

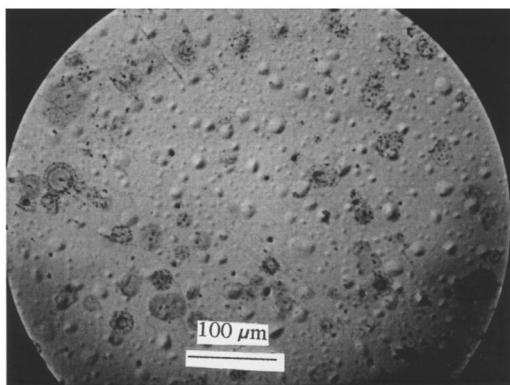


FIG. 6. Micrograph of sample 2 after 18 months of storage with blistering of the film evident. The sample originally had no visible features after film growth.

that sample had dropped significantly. We interpret this as indicating that the excess nitrogen species, present as point defects in the as-grown film, were able to migrate through the lattice, assisted by the grain boundary defects of this polycrystalline material, and either escape the material from the top surface or form bubbles at the substrate–film interface (this interpretation is to be discussed in more detail elsewhere¹⁶). In either case this would cause a drop in the N–N signal observed by SIMS.

The SIMS signal for the N–N species in the sample grown with a 1.92 eV band gap was a factor of 6 lower than for the as-grown sample 2 (see Fig. 5). This is consistent with the 1.92 eV sample having improved stoichiometry.

IV. CONCLUSIONS

With regard to the current controversy over the low band-gap InN observed for some MBE material,^{1–3} at this stage the large N/In ratios observed here do not appear to explain the difference between the 1.89–2.3 eV material and the apparent 0.7–1.5 eV values observed elsewhere, since all of the data is consistent with the 1.89 eV band gap previously observed²⁰ for near stoichiometric (1:1) InN produced by rf sputtering.

In conclusion, the experimental results presented here show that the high n -type carrier concentration for rf sputtered indium nitride is not due to nitrogen vacancies, and it further appears that excess nitrogen is possibly the source of the background n -type doping. Similar results may be expected for MBE grown material where excess nitrogen has also been observed. It has further been shown that oxygen content does not correlate to changes in the lattice constant of rf sputtered material, the incorporated oxygen is intergranular and does not contribute to the InN XRD. Instead, it has been demonstrated that previously undetected, and unexpected, variations in excess nitrogen content are responsible.

ACKNOWLEDGMENTS

K.S.A.B. would like to acknowledge the support of an Australian Research Council Fellowship. We would also like to acknowledge the support of the Australian Research Council through a Large grant and a Discovery grant; the support of a Macquarie University Research Development Grant, and the Australian Institute of Nuclear Science and Engineering for SIMS access. The authors are also indebted to C. Stampfl of Sydney University for useful discussions, and to W. Schaff of Cornell University for the supply of MBE grown InN samples.

¹T. Inushima, V. V. Mamutin, V. A. Vekshin, S. V. Ivanov, T. Sakon, M. Motokawa, and S. Ohoya, *J. Cryst. Growth* **227–228**, 481 (2001).

²J. Wu, W. Walukiewicz, K. M. Yu, J. W. Ager III, E. E. Haller, H. Lu, W. Schaff, Y. Saito, and Y. Nanishi, *Appl. Phys. Lett.* **80**, 3967 (2002).

³V. Tu Davydov, A. A. Klochikhin, V. V. Emtsev, D. A. Kurdyukov, S. V. Ivanov, V. A. Vekshin, F. Bechstedt, J. Furthmuller, J. Aderhold, J. Graul, A. V. Mudryi, H. Harima, A. Hashimoto, A. Yamamoto, and E. E. Haller, *Phys. Status Solidi B* **234**, 787 (2002).

⁴K. S. A. Butcher, M. Wintrebert-Fouquet, Motlan, S. K. Shrestha, H. Timmers, K. E. Prince, and T. L. Tansley, in the Material Research Society Fall 2002 Conference Proceedings (to be published).

⁵T. L. Tansley and C. P. Foley, *Electron. Lett.* **20**, 1066 (1984).

- ⁶V. W. L. Chin, T. L. Tansley, and T. Osotchan, *J. Appl. Phys.* **75**, 7365 (1994).
- ⁷C. Stampfl, C. G. Van de Walle, D. Vogel, P. Kruger, and J. Pollmann, *Phys. Rev. B* **61**, R7846 (2000).
- ⁸S. Limpijumnong and C. G. Van de Walle, *Phys. Status Solidi B* **228**, 303 (2001).
- ⁹T. L. Tansley and R. J. Egan, *Phys. Rev. B* **45**, 10942 (1992).
- ¹⁰M. R. Ranade, F. Tessier, A. Navrotsky, and R. Marchand, *J. Mater. Res.* **16**, 2824 (2001).
- ¹¹H. Timmers, T. D. M. Weijers, and R. G. Elliman, *Nucl. Instrum. Methods Phys. Res. B* **190**, 393 (2002).
- ¹²K. S. A. Butcher, H. Timmers, Afifuddin, P. P.-T. Chen, T. D. M. Weijers, E. M. Goldys, T. L. Tansley, R. G. Elliman, and J. A. Freitas, Jr., *J. Appl. Phys.* **92**, 3397 (2002).
- ¹³Afifuddin, K. S. A. Butcher, T. L. Tansley, H. Timmers, R. G. Elliman, T. D. M. Weyers, and T. R. Ophel, *The Properties of GaN Films Grown by Plasma Assisted Laser-Induced Chemical Vapour Deposition*, 2000 International Semiconducting and Insulating Materials Conference Proceedings (IEEE, Piscataway NJ, 2000), pp. 51–54.
- ¹⁴H. Timmers, T. R. Ophel, and R. G. Elliman, *Nucl. Instrum. Methods Phys. Res. B* **161–163**, 19 (2000).
- ¹⁵S. K. Shrestha, H. Timmers, K. S. A. Butcher, and M. Wintrebert-Fouquet, *Proceedings of the International Conference on Advanced Materials and Nanotechnology*, Wellington, New Zealand (2003), *Current Appl. Phys.* (to be published).
- ¹⁶S. K. Shrestha, H. Timmers, K. S. A. Butcher, and M. Wintrebert-Fouquet, *Nucl. Instrum. Methods Phys. Res. B* (to be published).
- ¹⁷H. Lu, W. J. Schaff, J. Hwang, H. Wu, G. Koley, and L. F. Eastman, *Appl. Phys. Lett.* **79**, 1489 (2001).
- ¹⁸S. Kumar, L. Mo, Motlan, and T. L. Tansley, *Jpn. J. Appl. Phys., Part 1* **35**, 2261 (1996).
- ¹⁹O. Lagerstedt and B. Monemar, *Phys. Rev. B* **19**, 3064 (1979).
- ²⁰T. L. Tansley and C. P. Foley, *J. Appl. Phys.* **59**, 3241 (1986).
- ²¹W. Paszkowicz, R. Cerny, and S. Krukowski, *Powder Diffr.* **18**, 114 (2003).
- ²²C. Stampfl, Sydney University, Australia (private communication).
- ²³Y. Gao, *Surf. Interface Anal.* **14**, 552 (1989).